CORONAL DIAGNOSTIC SPECTROMETER
SoHO

CDS SOFTWARE NOTE No. 51

Version 1 16 June 1998

The VDS Burn-in Calibration

William Thompson
NASA Goddard Space Flight Center
Code 682.3
Greenbelt, MD 20771

William.T.Thompson.1@gsfc.nasa.gov

1 Introduction

The detector used within the CDS Normal Incidence Spectrograph (NIS), known for historical reasons as the Viewfinder Detector Subsystem (VDS), uses a microchannel-plate intensifier to detect the EUV photons, and convert them into visible radiation which is then collected by the CCD. As the detector is exposed to radiation, it will slowly decrease in amplification, through a process known as scrubbing. The design of the NIS is such that emission lines will always fall on the same location on the detector. Those pixels on the detector which correspond to the strongest lines will receive the largest dose over time, and the lose of sensitivity will be greatest in these areas. We say that these strong lines get burnt into the detector.

There are three aperture slits which are most commonly used with the NIS. Two of these, slit #4 and slit #5, are narrow slits of dimensions $2'' \times 240''$ and $4'' \times 240''$ respectively, suitable for resolving spectral lines. Because of the resolution of the NIS spectrometer, the primary differences between these two slits on the detector are spatial resolution and intensity—the observed line widths are very close to being the same. Approximately 95% of the NIS observations are made with one or the other of these narrow slits. The remaining 5% of the time, except for a few isolated cases, is spent observing with a wide $90'' \times 240''$ aperture (slit #6) suitable for obtaining spectroheliogram images in the stronger lines. Sometimes this wide slit is known as the "movie" slit, because of its use in making high cadence time series observations.

One of the benefits of the movie slit is that it allows the burn-in due to the more commonly used narrow slits to be directly observed and measured. Comparing Figure 1 with Figure 2 shows this quite clearly. Figure 1 is an observation made early in the mission, when little or no burn-in had occured on the detector. Figure 2 is a more recent observation.

2 Calibrating the narrow slit burn-in

In order to track the burn-in of the detector over time, a special study is run twice a week. This study, known in the CDS planning software by the acronym NIMCP, takes three exposures with the $90''$ movie slit at slightly different spatial positions, followed by a single exposure with the $2''$ narrow slit. The first step in the processing of these data is to remove all known detector effects are removed from the data, except the burn-in correction. The three movie-slit measurements are then averaged together to help wash out spatial features. To further wash out the effect of solar spatial variation, a number of NIMCP observations are averaged together, usually over about a two-week period. Finally, to help wash out any solar features which remain, the data are averaged in the vertical direction. The burn-in measured by this technique will then be an average value over the length of the slit. The same averaging procedure is also applied to the data taken with the narrow slit, except that here a correction is made for estimated burn-in effects.

The analysis of the resulting average profiles is a multistep process. First, a region of the spectrum is selected. The narrow slit spectrum from this region is then fitted to extract the intensities in each line. These intensities are then used to develop a model of what the same spectrum would look like if observed with the movie slit. The model is then adjusted to fit to the observed average movie-slit profile, with the narrow slit burn-ins modelled with Gaussian functions. Figure 3 shows a sample window from the IDL[1] fitting program used to perform this analysis. The

[1] IDL is a registered trademark of Research Systems, Inc.

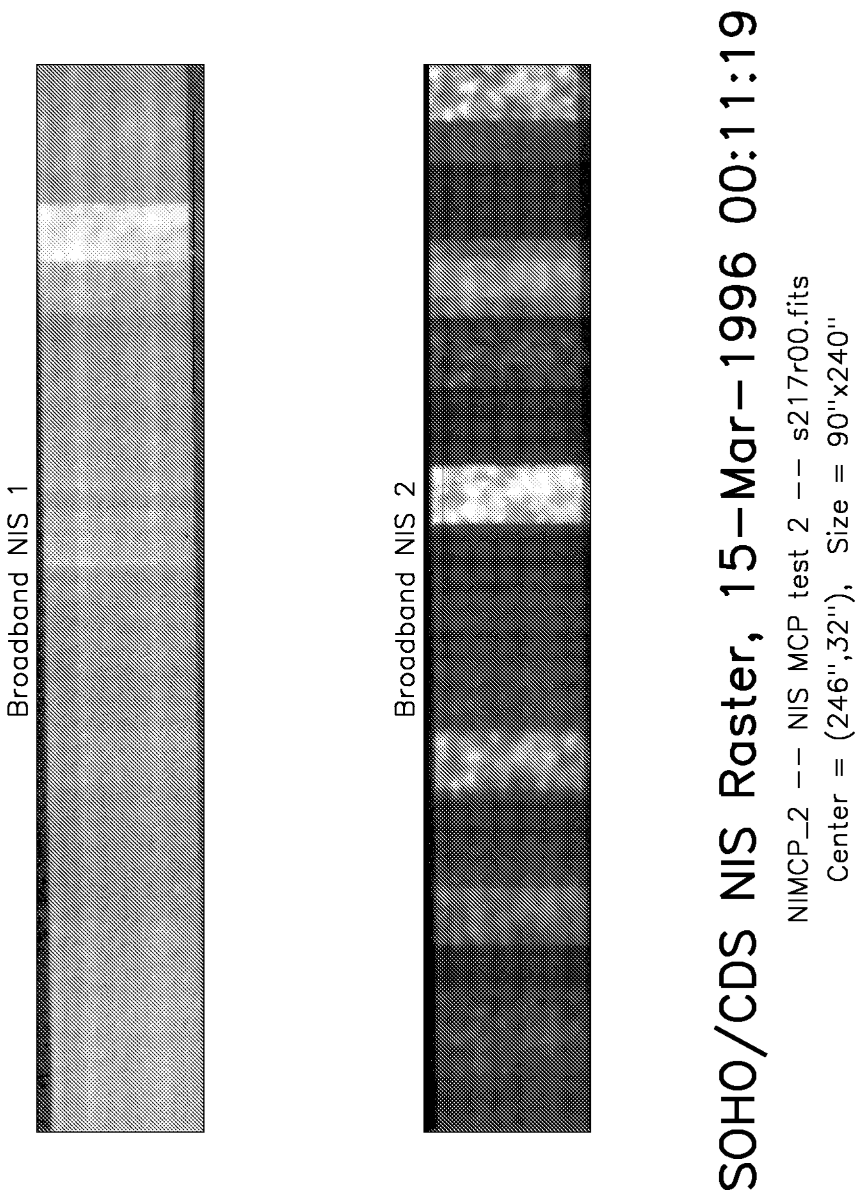

Figure 1: An observation from early in the mission, before any burn-in occurred. The CDS 90″ wide "movie" slit (#6) is used, showing spectroheliogram images where-ever there is a strong emission line.

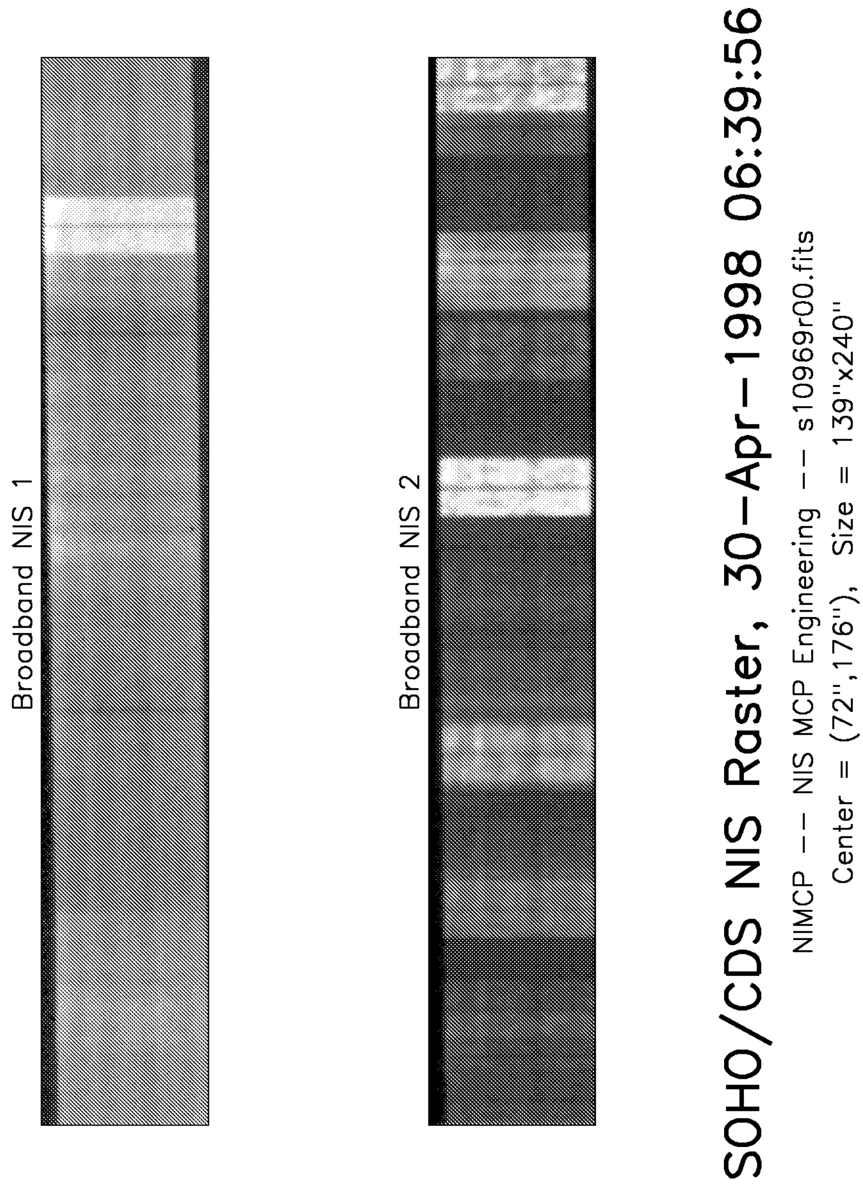

Figure 2: A recent observation, clearly showing the burn-in of strong lines. These burn-ins occur down the center of each strong spectroheliogram image, where the narrow slit spectral lines would illuminate the detector. Compare with Figure 1.

blue line shows the narrow slit profile from the dataset being analyzed. The green line is the fitted spectrum. Also shown, in brown, is a reference narrow slit profile derived from a much larger set of observations—this is used to indicate to the user activity-associated lines which might not appear in the present dataset. Note, for example, that the line at 520.7Å is much lower in the observation than in the reference spectrum. In some observations, it does not appear at all. The yellow line is the observed movie slit profile, and the red line is the fit to this profile. The vertical dashed lines mark the limits of the range considered in the fit represented by the red line. The dotted vertical lines are simply aids to the user to point out expected locations of lines.

Fitted burn-in parameters from a series of such analyses over the lifetime of the mission leads to plots like those shown by the "*" symbols in Figure 4. This plot shows the burn-in due to the exposure of the detector to the very strong He I line at 584Å, which is the strongest line observed by the VDS, and consequently shows the greatest amount of burn-in. It was found that most of the lines could be well fitted with a curve of the form

$$\beta = a_0 + a_1 \exp(-\Delta t / a_2) \tag{1}$$

with the constraint that $\beta \leq 0$. Expressing the data by an empirically-derived analytical curve allows the data to be interpolated or extrapolated to any date. For some of the stronger lines, such as the 584Å line shown in Figure 4, two curves were joined together to adequately replicate the behavior of the data points. The RMS differences between the measured data points and the fitted curve are typically on the order of 3% or less, and appear to be randomly distributed.

Table 1 shows the list of all lines with known burn-ins of their narrow slit profile, together with their central burn-in depths as of 4 April 1998. The CDS calibration routines `VDS_CALIB` or `NIS_CALIB` will automatically correct the data for these burn-in profiles. Figure 5 shows the effect of this correction on the same data shown in Figure 2.

The amount of burn-in of most lines can be correlated to their intensity in an average quiet sun profile. For example, the line with the strongest amount of burn-in, at 584Å, is also the line which is typically the strongest in any observation. The same goes for the O V line at 630Å. However, there are a few lines which show significant amounts of burn-in even though these lines are not particularly strong in the quiet sun, or may not even be present at all in some observations. The case of the line at 520.7Å has already been discussed. This line is produced by Si XII, which is relatively weak in the quiet sun, but becomes very strong in active regions. Other lines which show significant amounts of burn-in, but are faint or non-existent in quiet sun observations, are the Fe XVI lines at 335.4Å and 360.8Å. The significant amounts of burn-in which are seen at these line locations can only be attributed to exposure to active regions, where those lines become very strong. The 335.4Å line is a particularly good example of this. In the quiet sun, this line is blended with a cooler Mg VIII line at 335.2Å, which indeed usually dominates in the quiet sun. However, the location of the burn-in is clearly centered on the Fe XVI line, showing that it is active region observations which is producing the burn-in.

3 The flat field calibration

Another observation which is useful for measuring the amount of burn-in on the detector is FFCAL. Like NIMCP, this program observes with the 90″ wide movie slit. However, instead of telemetering down the entire NIS spectral ranges, seven data windows in the brightest areas of the spectra are selected for telemetry. This allows more rapid turnaround between exposures, and many more

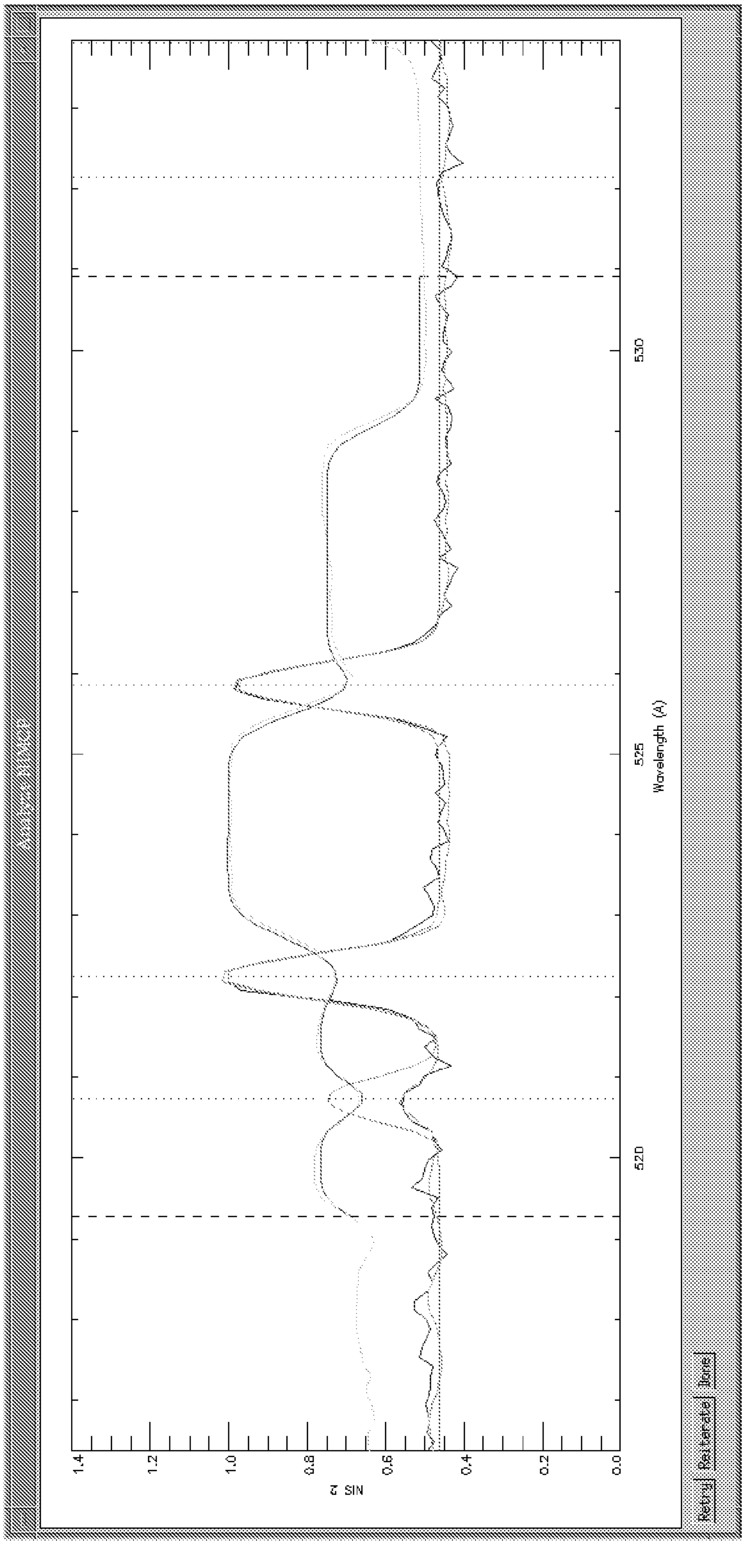

Figure 3: Sample window from the burn-in fitting program. See the text for an explanation of the colors.

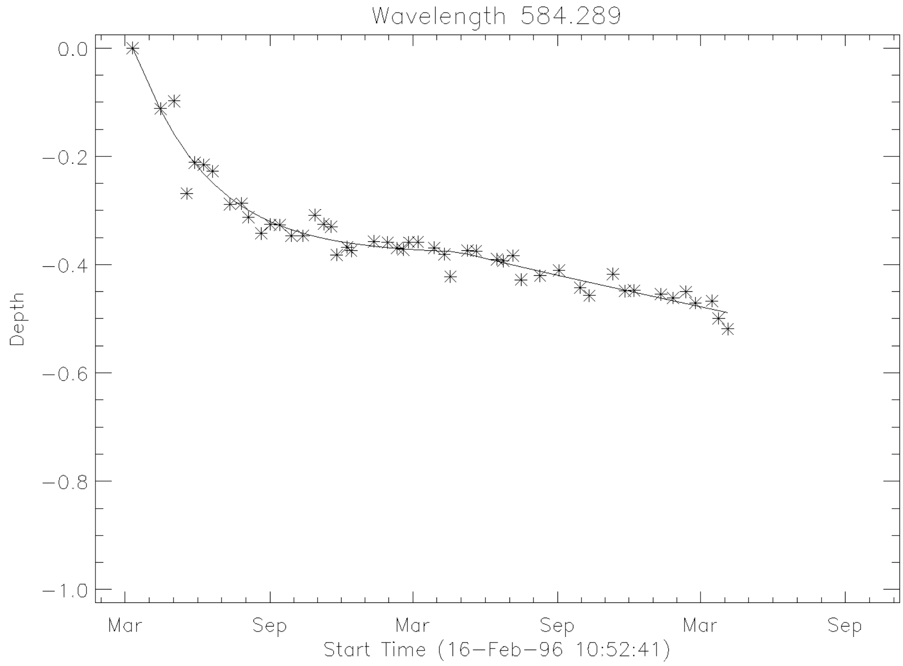

Figure 4: Burn-in measurements of the He I line at 584Å, where 0 represents no burn-in, and -1 represents complete burn-in. The "*" symbols show the measured burn-in values, and the curve shows an empirical curve fitted to the data. This line is the strongest line observed by the VDS, and shows the greatest amount of burn-in.

Wavelength	Burn-in	Wavelength	Burn-in
315.0	-0.063	520.7	-0.224
334.2	-0.068	522.2	-0.087
335.4	-0.240	525.8	-0.135
342.0	-0.040	537.0	-0.221
345.1	-0.058	538.2	-0.070
349.9	-0.070	553.4	-0.099
352.1	-0.065	554.4	-0.305
352.7	-0.063	555.3	-0.081
356.0	-0.094	562.8	-0.094
360.8	-0.200	568.3	-0.087
364.5	-0.111	572.3	-0.066
367.8	-0.066	574.0	-0.063
368.1	-0.284	584.3	-0.489
		599.5	-0.182
		607.5	-0.232
		609.7	-0.339
		624.9	-0.256
		629.7	-0.442

Table 1: Lines with known narrow-slit burn-ins as of 4 April 1998.

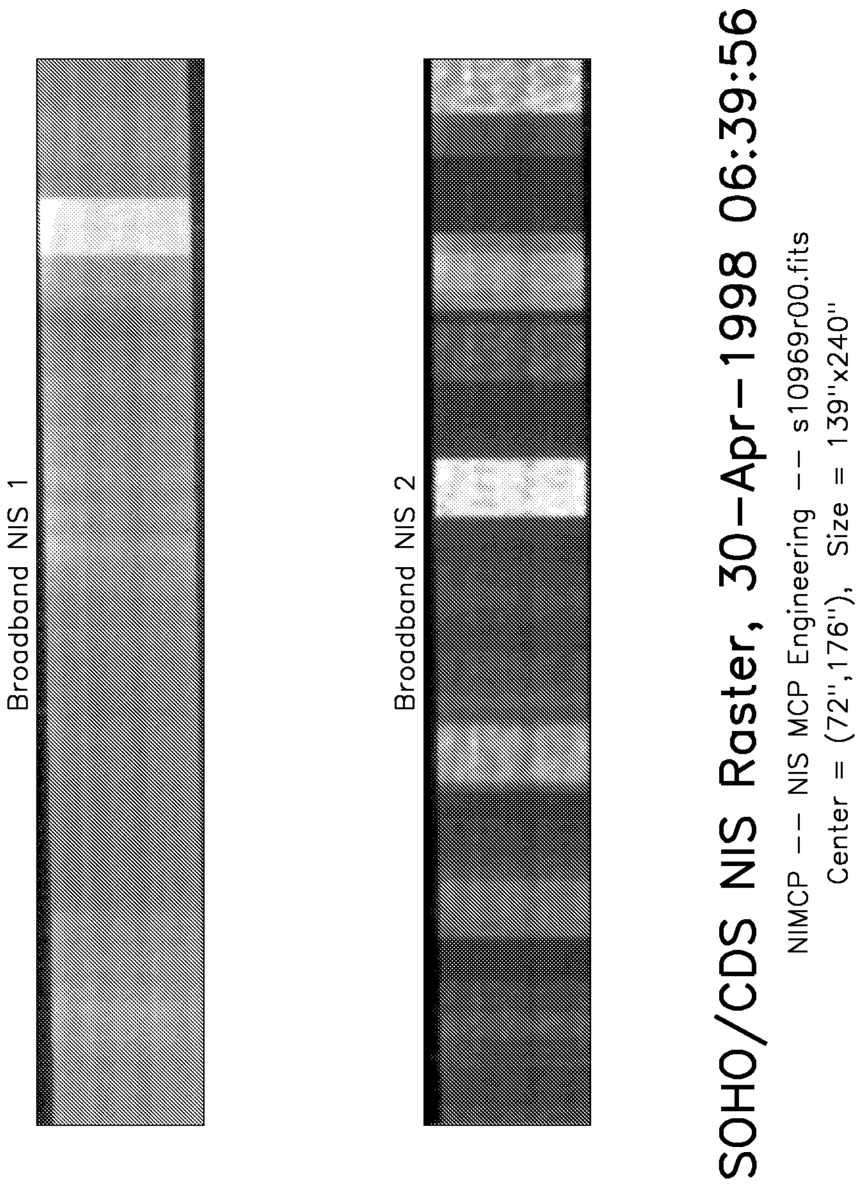

Figure 5: The data of Figure 2 after the narrow-slit burn-in correction has been applied.

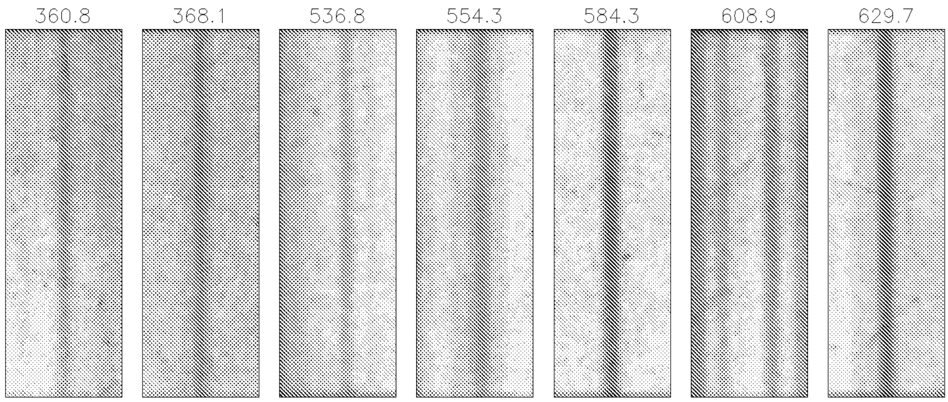

Figure 6: The response of the VDS detector to an essentially flat radiation field, in seven selected data windows. The effect of a flat radiation field was simulated by averaging together a number of exposures where solar features were smeared out by moving the instrument during the exposure. As well as the narrow-slit burn-in patterns of strong lines, one can also see the hexagonal pattern of the fiber-optic output window of the image intensifier.

exposures are taken in the same amount of time. During the run of the study, the CDS pointing mechanisms are slewn back and forth. This will cause some of the exposures to be taken while the instrument is in motion, resulting in a smeared image on the detector. By averaging together only those exposures which show a smeared sun, an essentially flat exposure image is built up in each data window, as demonstrated in Figure 6

The FFCAL observations are less frequent than the NIMCP observations, and don't cover all the lines with burn-in. However, the signal-to-noise in these images are much higher, and are less sensitive to solar features. They help refine the results of the NIMCP measurements, and also serve as a useful testbed for the burn-in correction algorithms. In particular, the FFCAL measurements are useful for determining the behavior of the shape of the burn-in profile with time.

4 Burn-in line profiles

As spectral lines get burned into the detector, the cores of the lines will burn in faster than the line wings. This will cause uncorrected line profiles to not only decrease in strength, but also slowly increase in apparent width. By modeling the burn-in with a Gaussian profile, this differential affect across the line should be accounted for, and the original line profile should be restored.

Detailed analysis of the burn-in line profiles show that in the lines with the greatest amount of burn-in, the profiles start to deviate from a Gaussian. This is caused by the fact that the burn-in of the line cores will start to slow down after reaching a depth of ~30% (*c.f.* Figure 4), while the wings of the line are still going down. In part, this effect is modeled by allowing the burn-in widths to increase with time. However, this does not entirely replicate the behavior of the burn-in profiles.

In a strongly burned in line like 584Å, a correction algorithm based on Gaussian profiles will restore the original solar intensity in the core of the line, but undercorrect in the line wings. The discrepency between the estimated intensity in the line cores, and the solar intensity is on the order of 2%. This has the effect of artificially narrowing the line profile.

In order to improve the burn-in line profiles, the Gaussian function must be modified to include a flattening parameter. Analysis of FFCAL observation shows that a function of the form

$$\begin{aligned} \sigma' &= \frac{2\sigma}{1+\sqrt{1+2|f|/\ln 2}} \\ z &= (x-x_0)/\sigma' \\ w &= z^2/(|f|+|z|) \\ y &= \beta e^{-w^2/2} \end{aligned} \qquad (2)$$

appears to well describe the behavior of the more strongly burned in lines. The parameters β, x_0, and σ are the normal Gaussian parameters describing the depth, position, and width. The additional parameter, f, describes the amount of flattening. When f is zero, then $\sigma' = \sigma$, $w^2 = z^2$, and one obtains the normal Gaussian formula. The transformation from σ to σ' is done so that the width parameter σ is directly comparable to that of a normal Gaussian. The full-width-half-maximum of a profile given by equation 2 will be independent of the parameter f. More work is needed to show how f varies with time. For the present, it is assumed that f is constant with time, which is consistent with the data that we presently have.

There appears to be some evidence that the center location of the burn-in profiles has shifted with time. This is most easily seen with the FFCAL observations, where the center positions of burn-in patterns due to the 584Å and 630Å lines both appear to have shifted by 0.3 pixels between September 1996 and May 1998. However, because there were no runs of FFCAL between September 1996 and September 1997, it's difficult to tell exactly how the position changes with time. For example, is this shift best modelled by a linear function, or as an event? There's also some indication of a shift in the NIMCP measurements, toward the long wavelength end of the NIS 2 spectrum. At the present, we model the shift with a linear fit.

Even with the best modelling of the burn-in shapes based on movie slit data, there's still a strong signature of the burn-in in the measured spectral line widths with time. This effect is greatest in the 584Å line, where the average width has descreased by ~8% since the beginning of the mission. Evidently, the shapes as measured by using the movie slit do not entirely represent the situation when one of the narrower slits is used. One possible explanation lies in the resolution of the detector itself. There's a small loss of resolution between the output of the MCP wafer and the phosphor, and also in the transfer lens between the fiber-optic output window and the CCD. This may distort the appearance of the burn-in profile seen when the movie slit is used, particularly in the wings.

5 Spatial variation along the slit

All the analysis of narrow-slit burn-in effects so far considered has assumed that the time-averaged behavior will be such that each part of the slit will receive a uniform dosage. Detailed examination of the data shows that this assumption holds for most of the lines. The exceptions are those lines whose burn-in values can be attributed to active regions, e.g. Fe XVI 335.4Å and 360.8Å. In those lines, there is a slight increase in the amount of burn-in in the center of the slit, suggesting that active regions tend to be selectively centered on the detector. A future version of `VDS_CALIB` will need to take this effect into account.

6 The effect of the movie slit

The CDS synoptic program consists of nine NIS rasters covering the solar meridian from the north pole to the south pole, in four lines: He I 584.3Å, O V 629.7Å, Mg IX 368.1Å and Fe XVI 360.8Å. This program is run each day, and thus offers the opportunity to monitor the long term variation in the CDS sensitivity.

Gaussian profiles were fitted to the average line profiles for each of the nine synoptic image sets each day. For each line, the median of the nine daily intensity values was extracted. This median value should be less sensitive to solar activity and coronal holes than any of the individual positions. Figure 7 shows the daily median values of the 584Å line. The open circles are for data without the narrow slit burn-in correction, and the filled circles are for the same data with the correction applied. (The initial data points, prior to mid-June of 1996, are slightly affected by a different readout mode of the CCD.) Although the correction does make a significant difference in the derived intensities, there is still a slow drift down, even after the correction has been applied. Another instrument on SOHO, the Solar EUV Monitor, measures the absolute irradiance of the sun in a band dominated by the related He II 304Å line. These data show no such variation over this period, which suggests that the variation seen in Figure 7 is not solar in nature. The O V 629.7Å line, which is the second strongest line seen by VDS, shows similar behavior, although less strongly. No such long-term effect is seen in Mg IX 368.1Å, although because of the high formation temperature of this line, it is more sensitive to solar variability which confuses the analysis. (The Fe XVI line is associated with strong solar activity, and thus is not conducive to this kind of analysis.)

It appears that there is an additional component to the loss of sensitivity in the VDS detector, besides the narrow-slit burn-in. One possibility is that there is an additional burn-in component from the use of the 90″ wide movie slit. This is supported by the fact that the residual sensitivity loss appears to be related to line strength.

The use of the movie slit accounts for less than 5% of the total accumulated exposure time of the VDS detector. However, its effect on the detector can be greater than the same amount of exposure from the narrow slit. This is because the narrow slit line profiles are spread over several pixels, and the burn-in effect is correspondingly diluted. With the 90″ wide movie slit, each pixel receives the full line intensity.

In order to estimate the effect of the movie slit on the detector, one must first estimate what the intensity would be if there were no loss of sensitivity. Unlike the narrow slit case, there is no completely unambiguous way to do this. One way to do this is to extrapolate the data in Figure 7

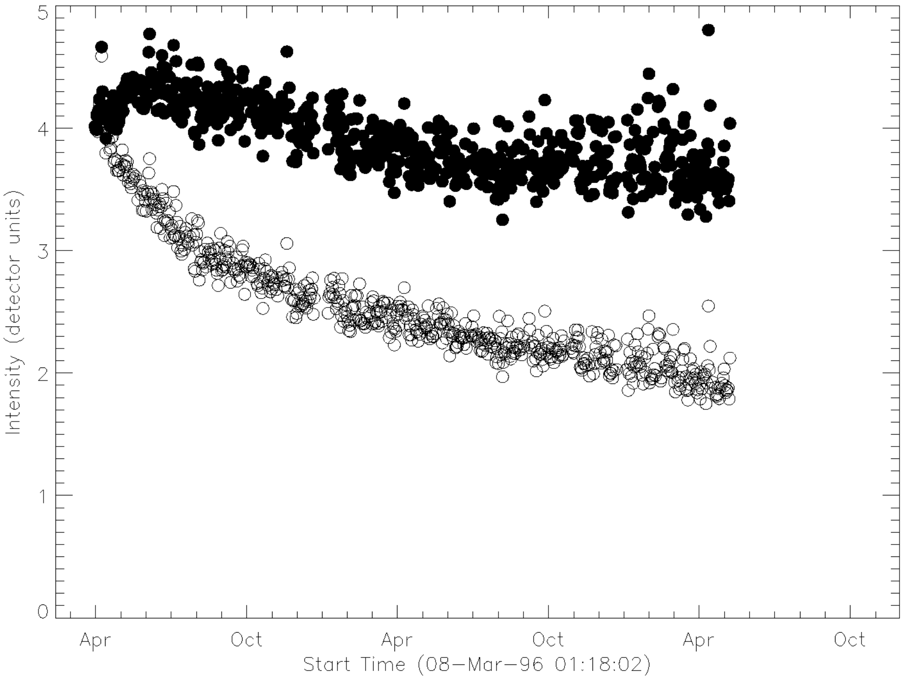

Figure 7: The median intensity values of the He I 584Å line, derived from the daily synoptic images. The open circles are the data without the narrow-slit burn-in correction applied, and the filled circles are with the correction applied.

to a date when regular observations with the movie slit began. Figure 8 shows the accumulated exposure time of the VDS detector with the movie slit. Up until about August 1997, the total exposure time is increasing roughly linearly. Superimposed is a dashed line showing a linear fit to the initial portion of the curve. It intersects the Y-origin on 21 March 1996, roughly near the end of the SOHO commissioning phase. The undisturbed average intensity of the He I 584Å line is estimated by extrapolating the data in Figure 7 to this date, using a fit to Equation 1.

In order to extrapolate the behavior of the 584Å line to other areas of the detectors, an average quiet-sun profile was built up from a number of movie-slit observations. These observations were selected from the earliest part of the mission, so that they themselves should not be affected by any loss of sensitivity over time. The average derived profiles are shown in Figure 9, normalized to unity at 584Å. (Some smoothing has been applied.) For any given pixel on the detector, the difference between the observation time and 21 March 1996 is multiplied by the normalized profile. This modified time is then inserted into Equation 1 with the parameters derived from Figure 7 to estimate the amount of wide-slit burn-in at that location.

To test the efficacy of this approach, another frequently run study is invoked. The NIS Spectral Atlas study, known as NISAT_S in the CDS planning software, obtains a complete spectrum in the two NIS wavelength ranges over a $20'' \times 240''$ spatial area. This study is run on a regular basis on a variety of targets. By selecting out those observations which are marked as quiet-sun in the CDS catalog, one can infer something about the long-term behavior of the detector at various pixel locations. This is similar to the analysis of the synoptic observations (Figure 7). However, because NISAT_S observes the complete NIS spectral ranges, many more lines can be evaluated.

If the supposition that the residual behavior of the 584Å line shown by the filled circles in

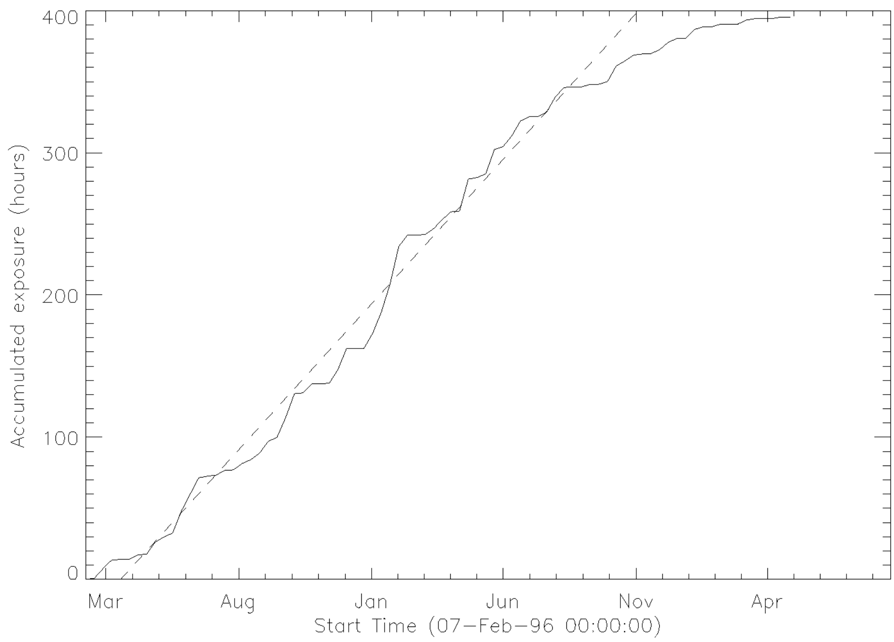

Figure 8: The accumulated exposure of the VDS detector to the 90″ wide movie slit. The dashed line is a linear fit to the earlier data.

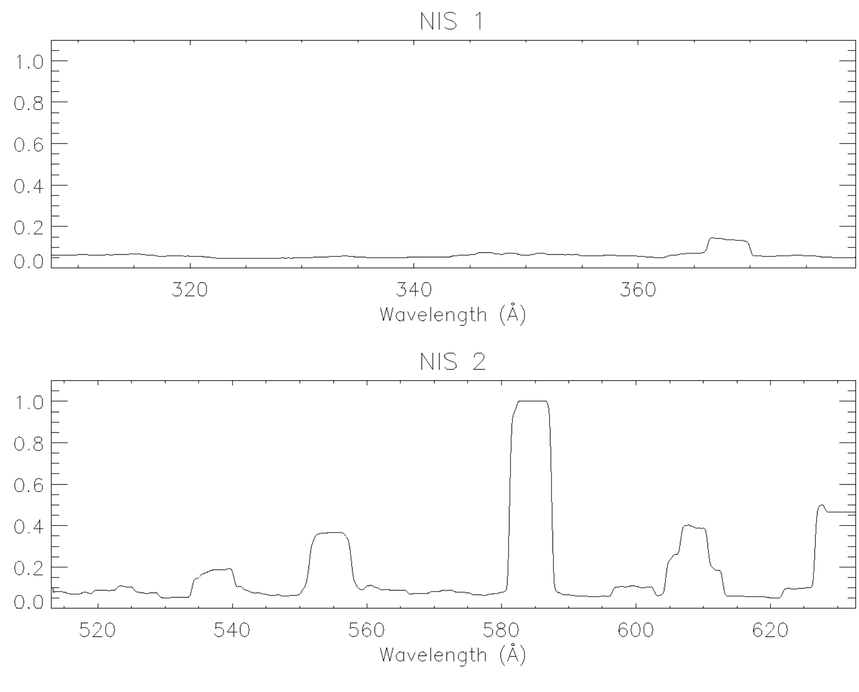

Figure 9: The average quiet-sun profile as observed with the 90″ wide movie slit. The data are normalized to unity at 584Å.

Figure 7 is caused by movie-slit exposure is true, then one would expect to see slow declines not only in strong lines, but also in lines close to strong lines. Unfortunately, the variation due to solar features appears to swamp out any such effect. At this point, all that can be said is that this approach appears to improve the stability of the 584Å and 630Å lines.

It should be noted that this approach does not take into account the increased exposure that some parts of the detector will encounter, such as around the Fe XVI lines at 335.4Å and 360.8Å, when observing active regions with the movie slit. Because most observations with the NIS only download selected data windows, there's no *a priori* way to build up an exposure history for each pixel. The exposure in the neighborhood of lines associated with hot plasma is also less likely to be smoothed out into a flat average exposure. For these and other reasons, active region observations with the movie slit are actively discouraged.

Because the measurement of the effect of the use of the movie slit on the VDS detector is indirect, and more problematical than the measurement of the narrow slit burn-in, this correction is currently optional in the VDS calibration software. One must specifically request it in the call to `VDS_CALIB`.

7 Conclusions

Most of the burn-in of bright spectral lines on the VDS detector can be tracked and removed, based on the analysis of movie-slit observations such as NIMCP and FFCAL. The accuracy of this process appears to be on the order of 3% or less. However, once this is done, the following artifacts still remain in the data:

- There is an additional suppression of bright lines which cannot be explained by the burning in of narrow spectral lines. It is theorized that this is due to the exposure of the detector to the 90″ wide movie slit, but has not yet been definitely confirmed. A crude correction for this effect can be applied by passing the `/SLIT6` keyword to `VDS_CALIB`, and is based on an average quiet-sun spectrum. The extra exposure in the regions around hot lines from active regions is not accounted for.
- The widths of strong lines show a narrowing over time after the burn-in correction has been applied. The narrowing shows a strong correlation with the amount of burn-in. This can be explained by an undercorrection in the wings of the line. The greatest amount of narrowing since the beginning of the mission is 8%, in the 584Å line.
- Some lines show a small amount of increased burn-in in the vertical center of the slit, evidently due to the practice of centering active regions within the field-of-view. This effect is not yet taken into account by the software.

As more information is determined about the burn-in, new calibration files will be generated. The most recent calibration file, as of this writing, is `$CDS_VDS_CAL_INT/nimcp_cal6a.dat`, which includes the best shape information as derived from FFCAL observations.